

## Supporting Information

### Grain Boundary Re-crystallization and Sub-nano Regions Leading to High Plateau

#### Figure of Merit for Bi<sub>2</sub>Te<sub>3</sub> Nanoflakes

Wei-Di Liu,<sup>ab</sup> Liang-Cao Yin,<sup>c</sup> Lei Li,<sup>c</sup> Qishuo Yang,<sup>d</sup> De-Zhuang Wang,<sup>c</sup> Meng Li,<sup>b</sup> Xiao-Lei Shi,<sup>b</sup> Qingfeng Liu,<sup>c</sup> Yang Bai,<sup>e</sup> Ian Gentle,<sup>f</sup> Lianzhou Wang,<sup>\*a</sup> Zhi-Gang Chen<sup>\*b</sup>

#### Section S1. Parallel model

The parallel model for electrical performance analysis of a composite material can be expressed as:<sup>1</sup>

$$\sigma_c = (1 - x_v) \cdot \sigma_m + x_v \cdot \sigma_v \quad (\text{S1-1})$$

$$S_c = \frac{(1 - x_v) \cdot \sigma_m \cdot S_m + x_v \cdot \sigma_v \cdot S_v}{(1 - x_v) \cdot \sigma_m + x_v \cdot \sigma_v} \quad (\text{S1-2})$$

$\sigma$  is the electrical conductivity,  $S$  is the Seebeck coefficient,  $x_v$  is the volume fraction of secondary phase (vacuum here),  $x_v=r$  ( $r$  is the relative density),  $c$  denotes for composite,  $m$  denotes for matrix, and  $v$  denotes for vacuum. When  $\sigma_v=0$  S cm<sup>-1</sup> and  $S_v=0$  μV K<sup>-1</sup> are taken into account, it can be extracted that:

$$\sigma_c = (1 - r) \cdot \sigma_m \quad (\text{S1-3})$$

$$S_c = S_m \quad (\text{S1-4})$$

As can be seen, the porosity  $r$  influence only the  $\sigma_c$  through vacuum compositing.  $S_c$  is still determined by the  $S_m$  of the matrix material.

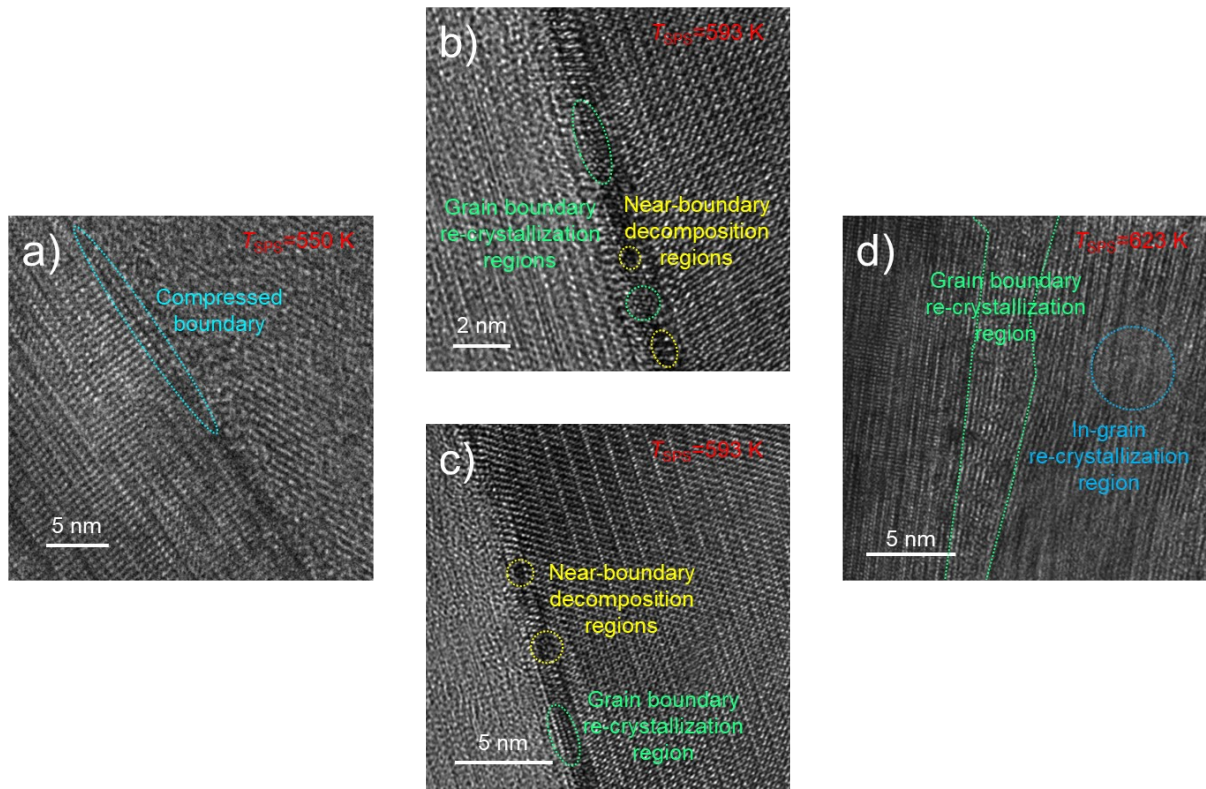


Fig. S1. High-magnification TEM images of as-sintered  $\text{Bi}_2\text{Te}_3$  pellets sintered under  $T_{\text{SPS}}$  of a) 550, b) and c) 593, and d) 623 K, respectively.

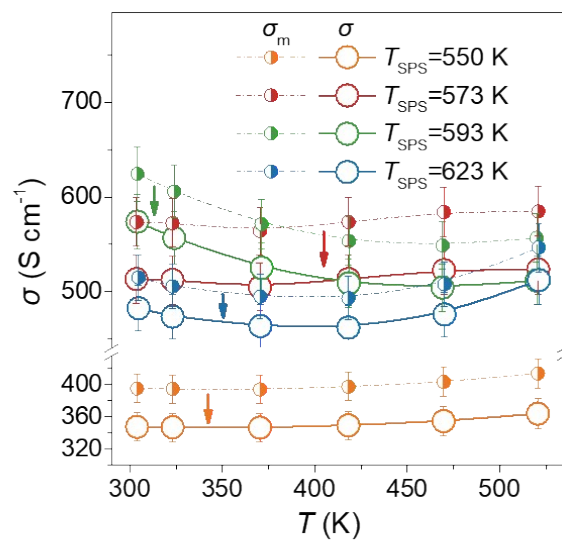


Fig. S2. Measured  $\sigma$  of as-prepared  $\text{Bi}_2\text{Te}_3$  pellets under different  $T_{\text{SPS}}$  in comparison with the  $\sigma_m$  extracted by parallel model.

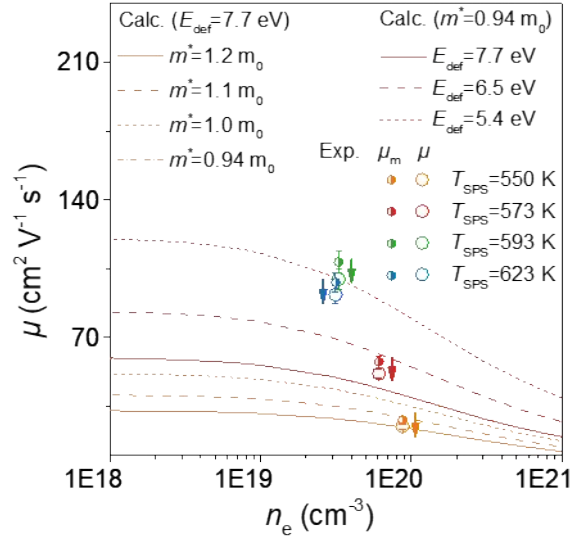


Fig. S3. Comparison between measured (under different  $T_{\text{SPS}}$ )  $\mu$ , extracted  $\mu_m$  and calculated (under different  $E_{\text{def}}$  and  $m^*$ )  $\mu$  as a function of  $n_e$ , at 370 K.

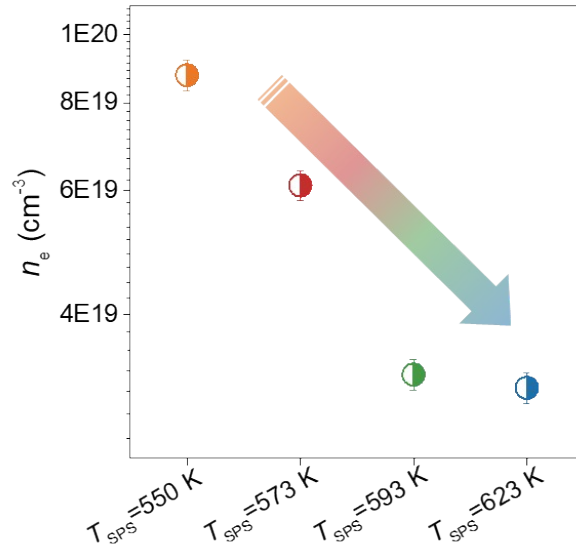


Fig. S4. Measured  $n_e$  of  $\text{Bi}_2\text{Te}_3$  pellets sintered under  $T_{\text{SPS}}$  of 550, 573, 593 and 623 K, respectively.

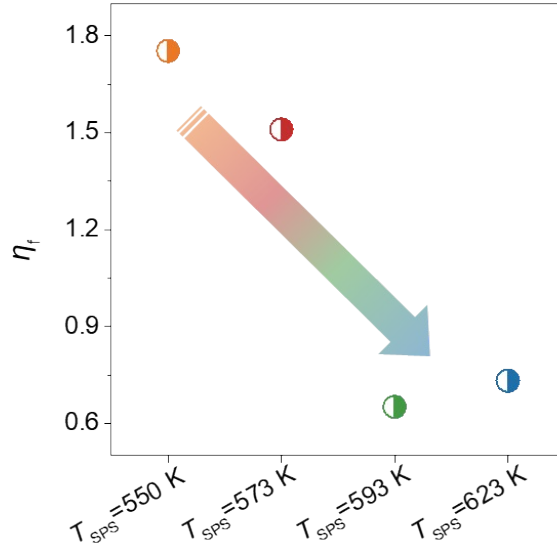


Fig. S5. SPB model extracted  $\eta_f$  of  $\text{Bi}_2\text{Te}_3$  pellets sintered under  $T_{\text{SPS}}$  of 550, 573, 593 and 623 K, respectively.

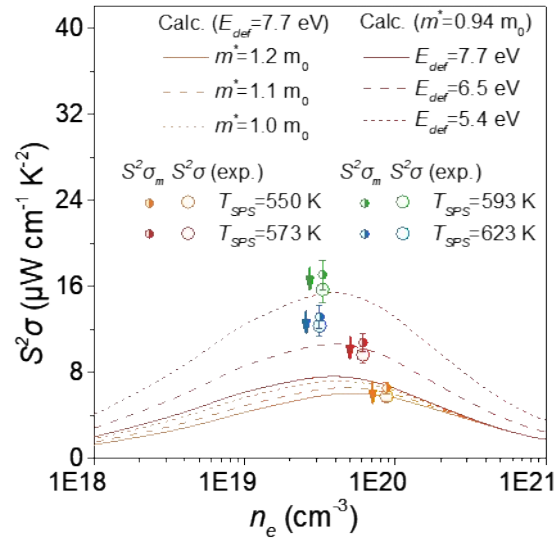


Fig. S6. Comparison between measured (under different  $T_{\text{SPS}}$ )  $S^2\sigma$ , extracted  $S^2\sigma_m$  and calculated (under different  $E_{\text{def}}$  and  $m^*$ )  $S^2\sigma$  as a function of  $n_e$ , at 370 K.

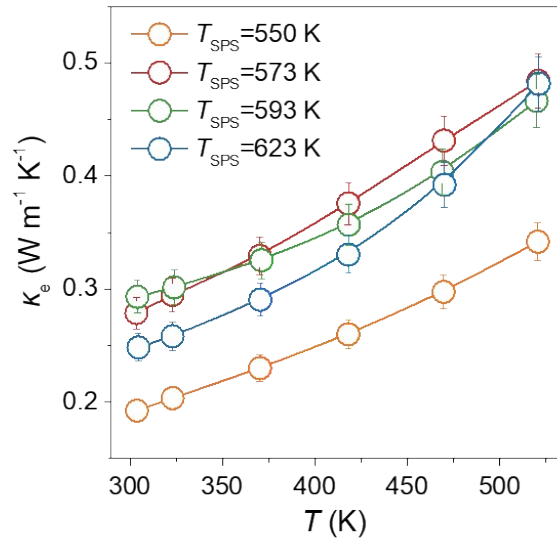


Fig. S7. Extracted  $\kappa_e$  of  $\text{Bi}_2\text{Te}_3$  pellets sintered under  $T_{SPS}$  of 550, 573, 593 and 623 K, respectively.

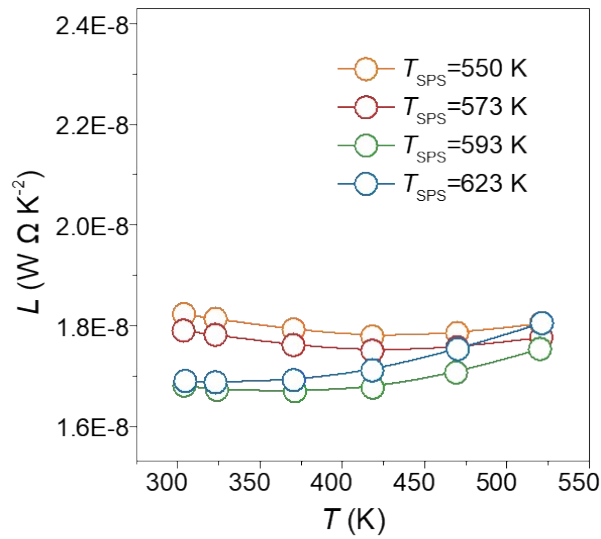


Fig. S8. Extracted  $L$  of  $\text{Bi}_2\text{Te}_3$  pellets sintered under  $T_{SPS}$  of 550, 573, 593 and 623 K, respectively.

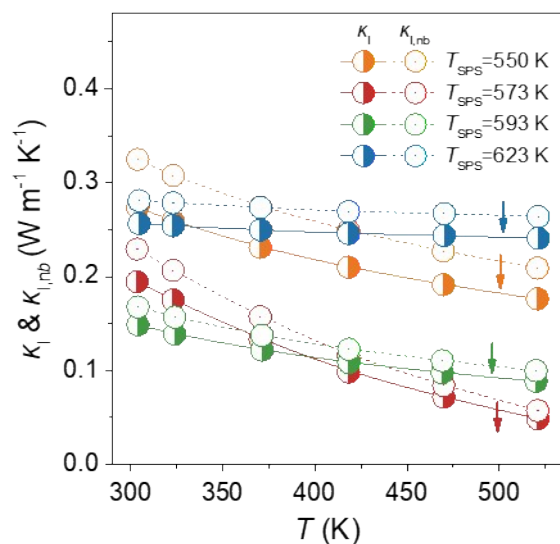


Fig. S9. Comparison between evaluated  $\kappa_1$  of  $\text{Bi}_2\text{Te}_3$  pellets prepared under different  $T_{\text{SPS}}$  and the gray medium model-evaluated  $\kappa_{1,nb}$  of nanobulks without pores.

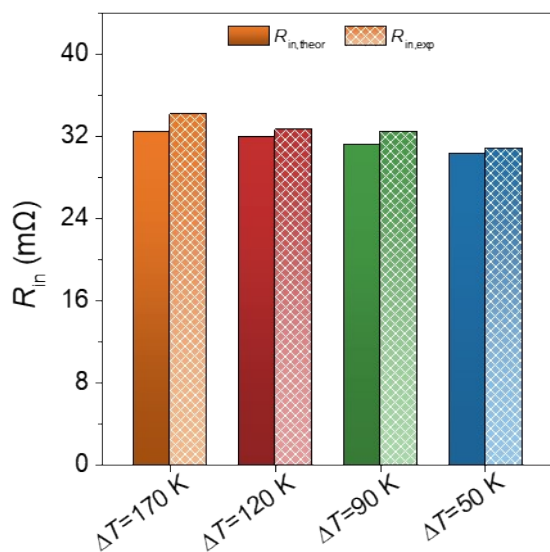


Fig. S10. Measured  $R_{\text{in}}$  of the of a single-leg device prepared based on the  $\text{Bi}_2\text{Te}_3$  pellet sintered under the  $T_{\text{SPS}}$  of 593 K under different  $\Delta T$ , comparing with the theoretical values.

Table S1. Comparison of key carrier transport properties evaluated by SPB model of  $\text{Bi}_2\text{Te}_3$  pellets prepared under different  $T_{\text{SPS}}$  and those of  $\text{Bi}_2\text{Te}_3$  matrixes (denoted by m) extracted by parallel model.

$T_{\text{SPS}}$ (K)	$n_e$ ( $\text{cm}^{-3}$ )	$\mu$ ( $\text{cm}^2 \text{V}^{-1} \text{s}^{-1}$ )	$\mu_m$ ( $\text{cm}^2 \text{V}^{-1} \text{s}^{-1}$ )	$m^*$ ( $m_0$ )	$m_m^*$ ( $m_0$ )	$E_{\text{def}}$ (eV)	$E_{\text{def,m}}$ (eV)
550	8.76E+19	24.7	28.1	1.17	1.17	7.68	7.20
573	6.11E+19	51.6	57.6	1.02	1.02	6.51	6.16
593	3.29E+19	99.6	108.4	0.94	0.94	5.44	5.22
623	3.15E+19	91.9	98.0	0.84	0.84	6.58	6.37

## References

1. H. Yao, Z. Fan, H. Cheng, X. Guan, C. Wang, K. Sun and J. Ouyang, *Macromol. Rapid. Comm.*, 2018, **39**, 1700727.